USE OF GLOBALLY AVAILABLE DATA FOR DETERMINING WATER LEVEL VARIATION IN LAKES: THE CASE STUDY OF LAKE TURKANA, KENYA

Charuni WICKRAMARACHCHI[1], Ioana POPESCU[2,3], Andreja JONOSKI[2], Jochen WENNINGER[4]

[1]UNSW Canberra, School of Engineering and Information Technology (SEIT), Canberra, ACT 2610, Australia
[2]IHE Delft Institute for Water Education, Department of Hydroinformatics and Socio-Technical Innovation, 2611 AX Delft, The Netherlands
e-mail: i.popescu@un-ihe.org
[3]Politechnica University Timisoara, Faculty of Civil Engineering, Department of Hydrotechnics, 300500 Timisoara, Romania
[4]IHE Delft Institute for Water Education, Department of Water Resources and Ecosystems, 2611 AX Delft, The Netherlands

DOI: 10.5281/zenodo.10376148

Abstract. This study identifies relevant globally available data to develop basin and water level variation models which can be used for scenario modelling. The case study for the current research is Lake Turkana in Kenya, which is the outlet of 3 main river basins: Omo, Turkwel and Keiro. Due to the lack of data, the present paper only considers the Omo River Basin, which contributes around 90% of the inflow into the lake. Lumped and semi-lumped hydrological models were developed using the USACE's HEC-HMS tool. The calibration and validation were carried out using the EU computed discharges of the Global Flood Awareness System as observed flow. The validated model was used to assess the impact on the lake due to the operation of three reservoirs in the basin; Gibe I, II and III. The variation of the water level of Lake Turkana was determined by using the model builder tool in ArcGIS. The lake water level model was validated using the Normalized Difference Water Index of Landsat 5 and Landsat 7 satellite imagery. Finally, using the semi-lumped hydrological model and the lake water level variation model, two scenarios were simulated to assess the lake's condition due to three consecutive driest and wettest years.

The semi-lumped model showed satisfactory goodness of fit compared to the lumped model, therefore it is concluded that it can be used to assess the impact of upstream developments in the Omo basin, on the shoreline and water level variations of Lake Turkana with reasonable accuracy.

Key words: Lake Turkana, hydrological modelling, Omo River Basin, remote sensing, HEC-HMS, lake water level variations, stakeholders competing interests, climate change

1. INTRODUCTION

Lake Turkana is an important lake located in the East African Rift Valley in the arid northwest of Kenya with its far northern end crossing into Ethiopia (Carr, 2017). The lake, surrounding basins, and bordering countries are shown in Figure 1a. This lake is known to be the world's largest permanent desert lake and the world's largest alkaline water body with a surface area of approximately 7560 km^2 (Obiero *et al.*, 2016). The overall basin area of Lake Turkana is approximately 130,860 km^2, and the lake has a mean depth of 31 m and a maximum depth of 114 m (Obiero *et al.*, 2016). The inflows into Lake Turkana are coming from the three major rivers: Omo, Turkwel and Keiro. The salinity level of Turkana Lake is unsuitable for human consumption or agricultural use, because the value is twice as much the one permitted by Kenyan water quality standards (Obiero *et al.*, 2016).

Currently, this lake faces a lot of challenges due to the stakeholders' increased demand for the water resources in the upstream of the catchment. The different stakeholders competing for the water are: hydropower, irrigation, fisheries and human consumption. As a result of these water uses the inflow into the lake is reduced considerably. Moreover, in Ethiopia the construction of the Gibe III dam in Ethiopia, Africa's tallest hydropower dam (approx. 244 m) could potentially cause a significant impact on the lake's inflow.

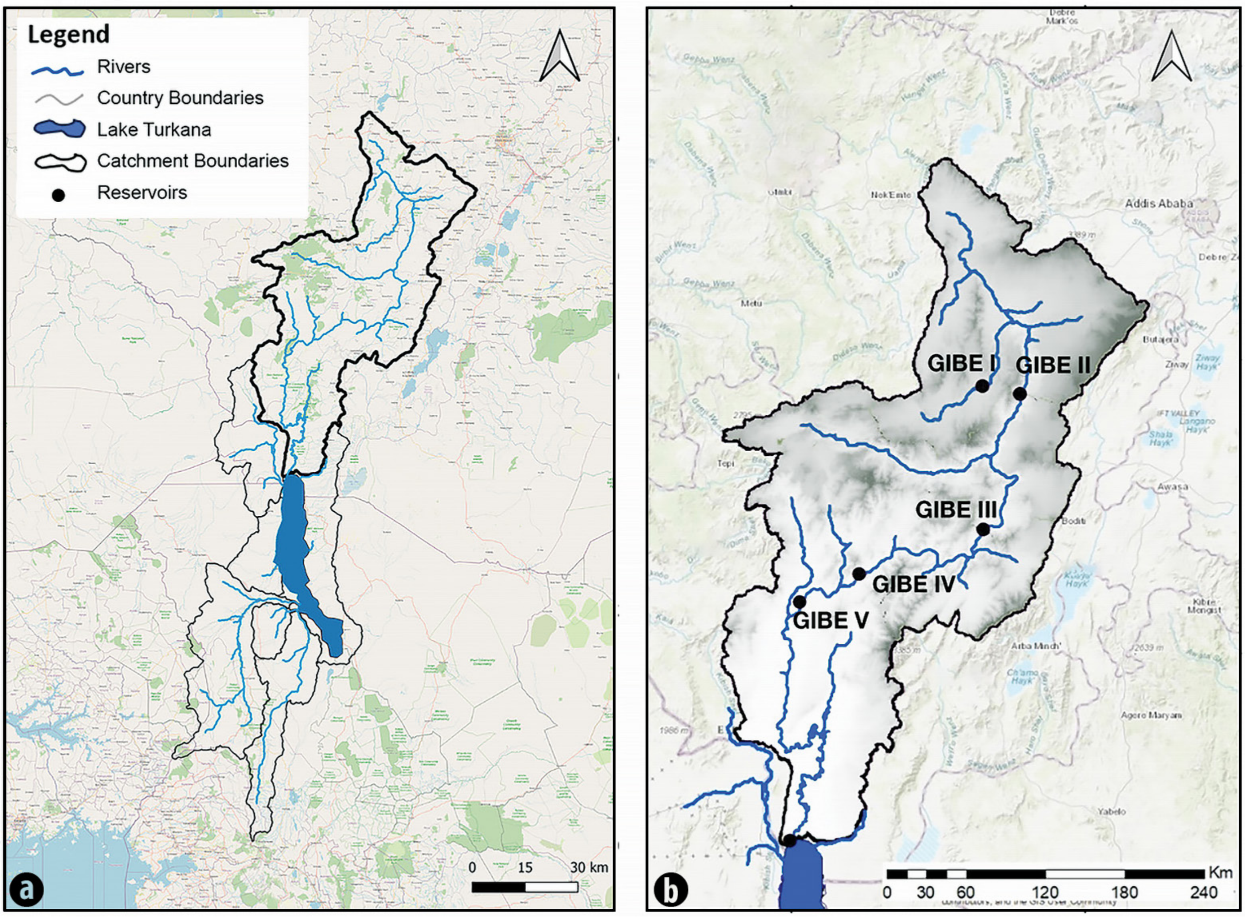

Fig. 1. Location of Lake Turkana. (**a**) Stream network and sub-basins and (**b**) Omo River Basin and Lake Turkana.

The Omo River which is flowing from the Ethiopian highlands provides over 90% of fresh water to the Lake Turkana. It is also the main source of nutrients for the lake and maintains the lake's productivity by controlling its salinity and altering the turbidity of the ecosystem (Kolding, 1992). The ephemeral Turkwel and Keiro Rivers contribute to the remaining 10% inflow to the lake. There are also a few other minor rivers and numerous streams that flow into the lake, with negligible influence on the hydrological balance of the lake. The only outflow from the lake is evaporation which is about 7.2 mm/day. It should be highlighted that as Lake Turkana basin is a data scarce study area, if not mentioned otherwise, the current study worked with data, such as evaporation as constant value, average discharge into the lake from minor rivers; as available in Avery (2010) and results obtained through research were compared with the same source. Avery and Tebbs (2018) mention that during 2015-2016, the lake's water level declined by 2 m while the Gibe III reservoir was filled. More concerning are the plans for large-scale irrigation in the lower Omo basin that can abstract around 50% of the river water, potentially leading to a permanent shrinkage of the lake. Lake Turkana is known to be an "allotropic riverine lake" due to its high dependency on the riverine nutrient inputs which are supplied by the Omo River (Obiero *et al.*, 2016). Therefore, any major changes in the upstream part of the lake would cause a significant reduction of inflow to the lake. This will lead to a reduction of its water level, which will in return reduce the water quality of the lake, negatively affect pastoral, agricultural and fishing livelihoods of thousands of indigenous people who are depending on this water in the downstream regions (Carr, 2017). The fisheries industry is a major source of income for these people as it employs about 3000 fishermen and yields over 4000 tons of fish per year which provides high-quality animal protein for them. Another main source of income is agro-pastoralism which together with fishery supports the livelihoods of about 300,000 Kenyans (Miriti, 2017). Moreover, the transboundary nature of the basin makes it very challenging to solve such socio-economic and environmental problems that could have negative impacts on Lake Turkana.

Another notable reason which brings challenges to this lake is the predicted climate change in the future, which may result in more drastic variations of wet and dry conditions, even without the impact of the above-mentioned human interventions in the upstream part of the Omo basin. According to the 2021 United Nations Environment Programme (UNEP) report, eight human settlements around the lake are prone to be inundated by flooding periodically and this would become more regular and severe due to the impacts of climate change. Moreover, historical data suggests that if the lake level recedes below a level of 362 m.a.s.l., which is considered a critical condition, one of the gulfs of Lake Turkana the Ferguson Gulf (Fig. 1a) – will dry out. The Ferguson Gulf is one of the major breeding grounds for fish and therefore of great importance. However, during the last 25 years, the lake has fluctuated between 360 and 365 meters above sea level (m.a.s.l.) and as a result, the water level has reached such low levels that the Ferguson Gulf has dried out destroying the most productive fishing areas (Obiero *et al.*, 2016). A drop in the water level will cause a reduction in the water volume and hence reduce the fish habitats, and available biomass, and will increase salinity levels through the concentration of salts. Therefore, if the lake water level decreases by 20 meters, the lake volume would halve, and, as a result, the salinity level would double creating negative impacts on the lake's fauna and flora. Despite the great importance of this lake and all the challenges faced by it, due to its remote location and the unavailability of reliable ground-measured datasets, this lake is the least studied of the Great Lakes of Africa (Velpuri *et al.*, 2012).

Hydrological models and lake water level models are good tools to be used to study the water availability and the behavior of the lake under different climate situations and operating conditions of the reservoirs in the basins around the lake. Data availability, however, is the main factor which determines the model performance. There are many regions in the world where water-related studies are not carried out due to the unavailability of ground-measured data. Remote sensing data is a solution for such issues as it is globally available and easily accessible (Ali *et al.*, 2023). Due to the wide variety of parameters measured by remotely sensed data (precipitation, land use/land cover, soil maps, satellite imagery, etc.), these have become a key source of data for mapping, agricultural and environmental resource management, weather forecasting, and global change research (Musa et al, 2015). These data are also available in various temporal and spatial resolutions which affect the level of accuracy of a hydrological model. Therefore, the current study aims to identify relevant globally available data sets to develop a basin and a water level variation model for Lake Turkana which can further be used to analyze strategies to manage the competing interests of stakeholders and the potential effects of changing climate. To achieve this aim, two research questions are addressed:

- What level of accuracy can be achieved in developing semi-lumped rainfall-runoff model of the Omo catchment, when the main sources of data are globally available data sources?
- How can the combined models be used for testing strategies/scenarios of hydrological conditions and water resources management?

2. CASE STUDY DESCRIPTION

The Lake Turkana Basin receives a mean annual precipitation amount of ~200 mm where over 80% occurs between March and November due to the biannual passage of the East and West African monsoons. The rainy seasons are also known as "short rains" between early March and early June and "long rains" between late September and early November (Johnson & Malala, 2009). Therefore, the major vegetation of the basin is desert scrub and has a very low potential for plant growth.

The Omo River Basin (Fig. 1b) has an average annual potential evaporation of 2100-2500 mm with a mean annual temperature of 24°-30°C. The northern end of the lake's terrain is flat with hills and is dominated by the inflows of the Omo River. This region is also the most densely populated area of the lake shore due to the perennial freshwater inflow, and opportunities for settled agro-pastoralism and fishing. The northern end is the most vulnerable area for flooding due to its flat terrain and the presence of a delta. The Omo River Basin has a climate that varies from a tropical sub-humid climate in the northern end of the basin located in the highlands of Ethiopia, to a hot arid climate in the southern end of the basin that is located in the semi-desert areas in Kenya. The annual rainfall varies from 1900 mm per year in the north/central areas of the Omo Basin to mostly less than 300 mm per year in the southern areas of the basin. The monthly rainfall variation in the Omo River Basin is very diverse as the north of the basin has a uni-modal rainfall seasonality and a bi-modal rainfall towards the mid and south of the basin (Asefa, 2011; Avery and Tebbs, 2018).

3. RESEARCH METHODOLOGY

The applied methodology for research followed five distinct steps: literature research; data collection, processing and analysis; development of hydrological models of the Omo basin; development of the Lake Turkana water level variation based on inflows determined by the hydrological model; and assessing the impact Assessing the impact on the lake's water level due to three consecutive wettest hydrological years and driest hydrological years under two scenarios.

Initially, to address the research questions, a literature review was carried out to investigate the availability of global data for Lake Turkana. Based on the available data, two hydrological models were developed; one lumped and one semi-lumped. The hydroloical models were developed using the Hydrologic Engineering Center-Hydrologic Modeling System (HEC-HMS Version 4.9) which was developed by the U.S Army Corps of Engineers. Both models were developed only for the Omo Basin as data was unavailable to calibrate other sub-basins of Lake Turkana.

The lumped hydrological model was developed to understand the basin behavior and determine the overall parameters characterizing Omo catchment. Further, a semi-lumped hydrological model was developed based on the previously obtained parameters. These parameters were used as initial values during the calibration of the semi-lumped hydrological model.

A water level variation model of the lake was developed in ArcGIS to assess the changes of the lake's shoreline due to variations of the lake's inflows and outflows. Because the Omo Basin contributes 90% of the inflows into Lake Turkana, to account for the remaining 10% of inflows, the discharge result of the hydrological model of the Omo catchment, at the outlet, was multiplied by a factor of 1.1. Hence, the lake water level variation model was developed taking into account the total inflows to the lake. The only outflow of the lake is the evaporation and it was considered to be a constant average value of 7.2 mm/day which was obtained by calculating the Penman Evapotranspiration for the Lodwar Meteorological Station in Kenya. The analysis showed that the evaporation did not vary significantly throughout the year and that the evaporation taking place from the lake's surface was similar to the basin's evaporation.

As the final step of the research, the developed semi-lumped hydrological model and the lake water level variation model were used to simulate two scenarios:

1. Scenario A: assuming that the initial level of the lake is at the lowest recorded water level;
2. Scenario B: assuming that the initial level of the lake is at the highest recorded water level

These two scenarios were carried out to investigate how the discharge and the shoreline of the lake vary due to the rainfall of the wettest and driest hydrological years.

3.1. Data Availability

The following open-source data sets were used for the Lake Turkana study.

3.1.1. Digital Elevation Models and altimetry data

The Digital Elevation Model (DEM) of the Lake Turkana Basin was obtained from the Shuttle Radar Topography Mission (SRTM) (NASA, 2022), at a spatial resolution of 30 m by 30m. This DEM was processed to calculate the slopes of the terrain, flow lengths, delineating watershed boundaries and stream networks.

Altimetry heights of Lake Turkana were obtained from two different sources: Kenya Marine and Fisheries Research Institute (KMFRI) and the Database for Hydrological Time Series of Inland Waters (DAHITI).

Altimetry heights obtained from the KMFRI are measured in the research station on the western shore of Lake Turkana at Kalokol, Lodwar for the period of 1988-2009, at a temporal resolution of one per month. The KMFRI data are recorded relative to the zero datum (i.e 365.4 m.a.s.l., he Hopson datum, which is the lake level of the year 1972). The KMFRI gauge data often showed anomalies with respect to satellite data.

The second data source for altimetry heights is obtained from remote sensed measured data available in the DAHITI for 1992-2021. This database was developed by the Deutsches Geodätisches Forschungsinstitut der Technischen Universität München (DGFI-TUM) in 2013 to provide water level time series of inland waters over all continents, except Antarctica. The accuracy of this data varies between a few centimetres for large lakes and a few decimeters for small rivers and the temporal resolution mainly depends on the altimeter satellites (for example 10 days for Jason-3 and 35 days for Envisat) and the number of tracks crossing the inland water body (Schwatke *et al.*, 2015).

The comparison between the two datasets for the lake's water level fluctuation, from Figure 2 shows a deviation of up to 2 m between the two data sets.

3.1.2. Lake water level variation

The Gilgel Gibe III dam (Fig. 1b) which was commissioned in January 2015 was expected to reduce the water level of Lake Turkana by 2 m during the filling of its reservoir and subsequent dampening of the lake's seasonal flood cycle. Moreover, the Gibe III dam has scheduled a 10-day artificial flood release during August/September (during the wet season) at a rate of approximately 1600 m^3/s.

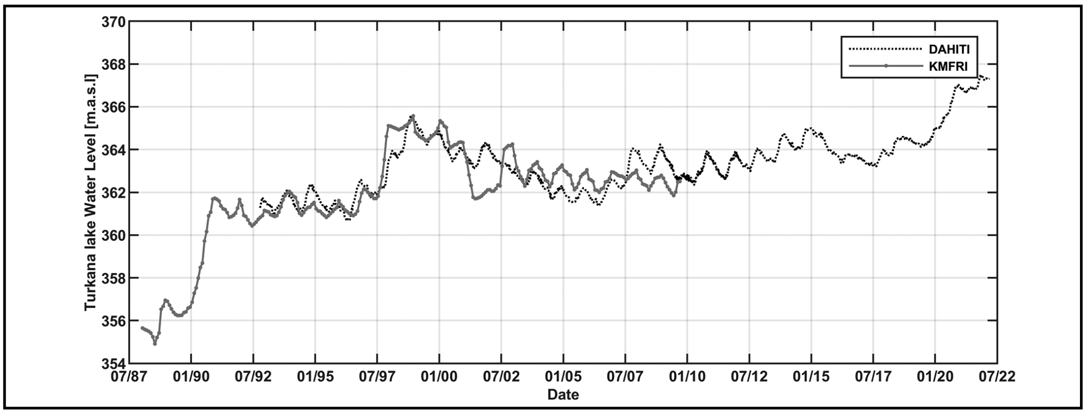

Fig. 2. Turkana lake water level variation.

This release was expected to decline the lake's average seasonal fluctuations from 1.1 m to 0.7 m (Gownaris *et al.*, 2017). In addition to reservoir operation, in the downstream areas of the Omo catchment, it is expected to cultivate over 200,000 hectares which will require 34% of the Omo River's annual inflow if the irrigation efficiency is 70% (moderate), or 44% of the Omo River's annual inflow if the irrigation efficiency is 45% (low). These water level fluctuations will significantly affect the fish population in the lake (Muška, *et al.*, 2012).

3.1.3. Rainfall

Multi-Source Weighted-Ensemble Precipitation data (MSWEP) (GloH20, 2022) is a global precipitation model providing data with a temporal timestep of 3 hrs. and a spatial resolution of 0.1°, available from 1979 to the present. MSWEP is produced by giving weight to different gauge and satellite data sources. The most often used gauge data are Climate Prediction Center (CPC) and Global Precipitation Climatology Center (GPCC), reanalysis from ERA-Interim and Japanese 55-year Reanalysis (JRA 55). Satellite data are available from Global Satellite Mapping of Precipitation (GSMap MVK) and TRMM 3B42RT (Chen *et al.*, 2020).

Climate Hazards Group InfraRed Precipitation with Station data (CHIRPS) (Climate Hazards Center, 2022) is a global precipitation model with data available from 1981 to the present. CHIRPS uses NOAA Climate Forecast System (CFS) reanalysis datasets to fill missing values calculated by gauged precipitation obtained from World Meteorological Organization's Global Telecommunication System and satellite datasets such as TRMM 3B42 (Chen *et al.*, 2020). As shown in Figure 3b, the rainfall pattern of the two data sets were very similar. CHIRPS data was used instead of MSWEP rainfall data for the rest of the research and this dataset is widely used for the Lake Turkana to produce accurate results (Avery and Tebbs, 2018, Christopher, 2014).

3.1.4. Soil Maps

Soil maps for the current study were obtained from the Soil Survey Geographic Database (SSURGO) which has a spatial resolution of 7.5 km (USDA, 2022). The SSURGO database contains information about the soils collected by the National Cooperative Soil Survey over a century. This soil data has been gathered by visiting the site, observing the soil and analyzing some of the samples in laboratories.

3.1.5. Land Use Data

Global Land Cover Characterization (GLCC) Land Cover Classification data (Earth Resources Observation and Science (EROS) Center, 2018) generated by the U.S. Geological Survey (USGS), the University of Nebraska-Lincoln (UNL), and the European Commission's Joint Research Centre (JRC) was obtained for the current study. This dataset has a spatial resolution of 1 km and is widely used in environmental research and modelling applications (Loveland *et al.*, 2000); Grekousis *et al.*, 2015; Sedano *et al.*, 2005).

3.1.6. Discharge Data

Discharge data for the current study was back-calculated using the two lake altimetry heights, KMFRI (available for 1988- 2009) and DAHITI (available for 1992- present) (Fig. 3). The back-calculated discharges were compared with the monthly averaged discharges available in Avery (2010).

The three discharge sources are described below.

(a) Back-calculated discharges using the water budget equation

The variation in the water level of Lake Turkana is the result of the total inflow from all the sub-basins, evaporation and precipitation over the lake. This concept was used to back-calculate the discharge using the altimetry heights over a selected computational time step (interval) using equation 1:

$$L_2 = L_1 - E_2 + P_2 + D_2 \quad (1)$$

where: L_1 is the water level at the beginning of the time step (m), L_2 is the water level at the end of the time step (m), E_2 is the evaporation during the time step (m), P_2 is the precipitation during the time step (m), and D_2 is the depth water level variation due to the total inflow into the lake (m). The depth water level variation (D_2) due to inflow was obtained by multiplying the inflow into the lake by the time step and dividing the obtained volume by the lake surface at the beginning of the calculated time step.

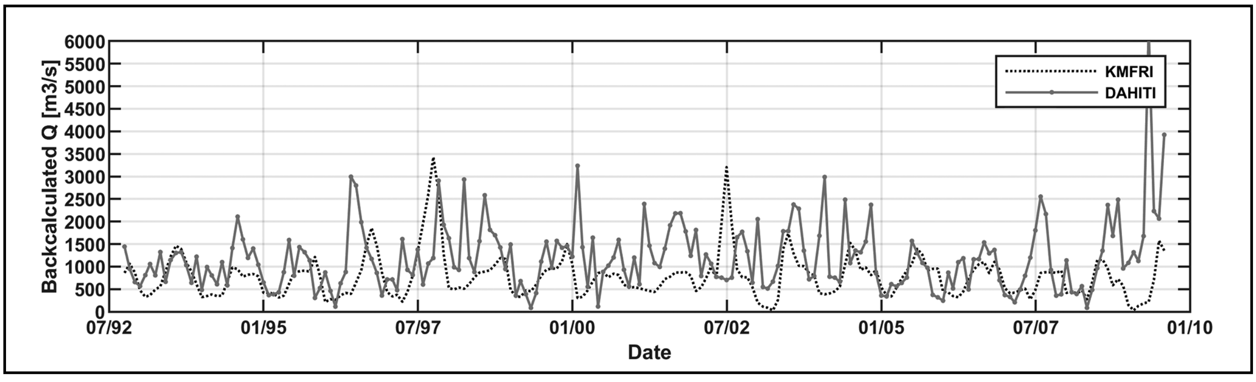

Fig. 3. Monthly averaged backcalculated discharges into lake Turkana, based on lake water levels of KNMFRI and DAHITI.

The computed water level L_2 was converted to a volume using a hypsographic curve developed for the Lake Turkana. All the levels were calculated by taking the datum to be 360.4 m.a.s.l

(b) Monthly average discharge data from the literature

Avery (2010) developed a hydrological model using measured monthly discharge data from 1977 to 1980 at a station located at the Omo delta (Omorate) to calibrate its model. The outcome of Avery (2010) report provides simulated monthly discharge data for the period 1956-1994.

(c) Global Flood Awareness System (GloFAS)

GloFAS is a global hydrological forecast and monitoring system which was jointly developed by the European Commission and the European Centre for Medium Range Weather Forecasts (ECMWF) (Copernicus, 2021). This system uses surface and subsurface runoff simulation results carried out by a surface model: HTESSEL (ECMWF, 2020) and a GIS-based spatially distributed hydrological model, Lisflood to simulate the groundwater and routing processes (van der Knijff *et al.*, 2010).

The historical discharge dataset was simulated by GloFAS by forcing the hydrological modelling chain with modelled gridded runoff data from the global reanalysis dataset (ERA5) (UN Environment Programme, 2020).

Figure 4 illustrates a comparison between the monthly average discharges obtained from GloFAS, literature and back calculated discharge from KMFRI data to determine the suitability of the datasets for calibration and validation purposes.

3.1.7. Reservoirs of the Omo River hydropower scheme

The Omo basin has a cascade of five dams, Gibe I, Gibe II, Gibe II, Gibe IV and Give V, as represented in Figure 1b (Avery and Tebbs, 2018). Gibe I is the first conventional hydroelectric power plant that was constructed in 1986 and was completed in 2004. The second hydropower plant, Gibe II, utilizes the water discharged by Gibe I as it is located downstream of Gibe I. Gibe III is very significant to the lake's water level as it would deprive the lake of 85% of its normal annual inflow in one year during the filling of its reservoirs and it requires almost 7% of the volume of water presently stored in Lake Turkana. During 2015-2016, when the reservoir of Gibe III was being filled, the lake's water level declined by 2 m. Two more hydropower schemes, Gibe IV and V, downstream of Gibe III were expected to add to the impacts of Gibe III. Contracts were signed in early 2016 to implement Gibe IV and it was expected to be commissioned in 2020. This project is downstream of Gibe III and approximately 580 km upstream of the lake (Avery and Tebbs, 2018). Gibe V is currently in the study phase.

3.2. Hydrological Modelling

Two hydrological models were developed; one lumped for the whole Turkana basin, to understand catchment behavior and one semi-distributed for Omo basin, to better represent the processes in the catchment. The second one was calibrated and validated using the backcalculated discharges.

3.2.1. Turkana basin lumped hydrological model

The study area was modelled as one lumped hydrological model using using the USACE's HEC-HMS tool. A sink element was used to represent the lake.

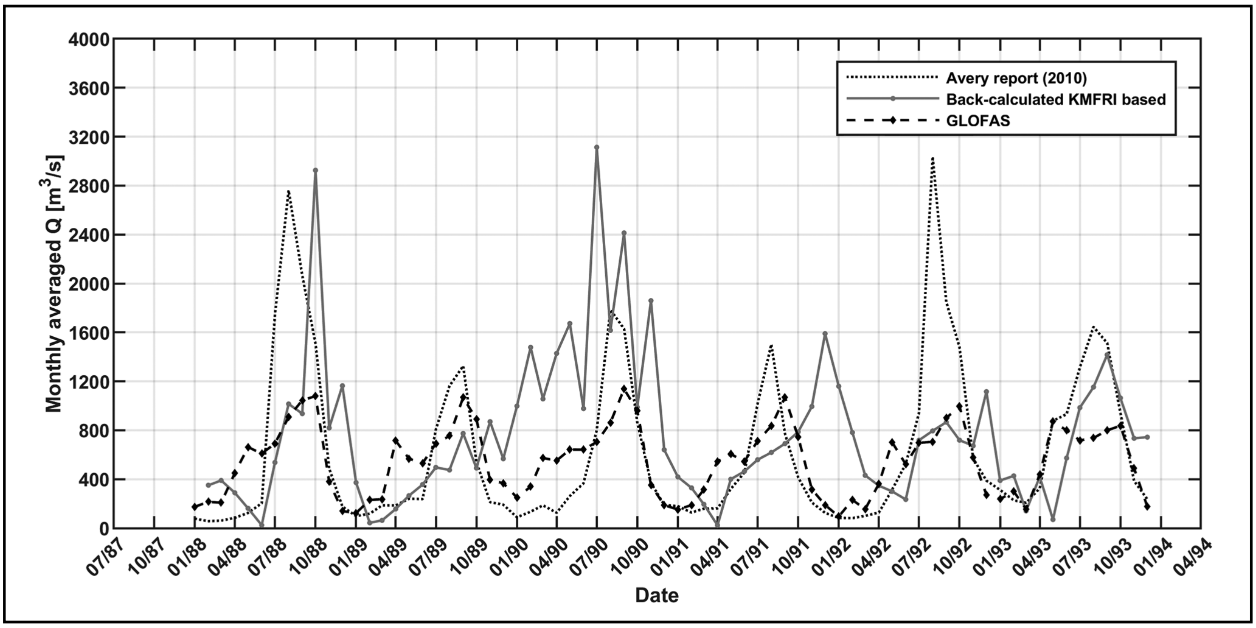

Fig. 4. Backcalculated discharge comparison with other data sources.

The lumped hydrological model did not consider the spatial variability of the parameters (canopy interception, impervious percentage, surface storage, infiltration, groundwater storage). The river network and the main Lake Turkana basin were obtained from the available DEM of the area. Three main rivers; Omo, Keiro and Turkwel, were considered, along with other 4 smaller rivers. Consequently, there are seven corresponding sub-basins (schematized in Figure 1a). The Omo sub-basin covers approximately 70,052 km^2 of the total area of the basin of the lake. The other six basins contribute less than 10% of the total inflow to the lake. Due to this insignificance of the flow and lack of data to model the other six sub-basins, the lumped model and the semi-lumped model were developed considering only the Omo basin.

A continuous simulation in daily time steps was carried out for calibration (1988-1993) and a similar one for the validation (1994-2000) of the model.

The considered components of the hydrological model are presented in Table 1.

Table 1. Components and methods of the lumped hydrological model

Component	Method used
Canopy	Simple Canopy method
Surface	Simple surface method
Loss	Soil Moisture accounting
Transform	Clark Unit hydrograph
Baseflow	Linear reservoir model

The initial canopy storage was estimated and the maximum canopy storage was averaged for each sub-basin based on the land use type, as defined by Bennet (2000).

The amount of surface storage depends on the slope and hollows and indentations of the ground surface. The weighted average slope of each sub-basin was categorized based on the slope ranges (Ouédraogo *et al.*, 2018).

The Soil Moisture Accounting Method represents the dynamics of water movement using five layers above and below the soil surface: canopy interception, surface depression storage, top soil, upper groundwater, and lower groundwater. The initial soil moisture and groundwater conditions were assumed based on the soil type, and the maximum infiltration was calculated by considering the weighted average of the saturated hydraulic conductivity of the topsoil. The impervious percentage was specified as a percentage of the area under urban civilization for each sub-basin. The soil storage, tension storage and soil percolation were calculated based on the weighted averaged porosity (top soil), available water capacity (top soil) and the averaged saturated hydraulic conductivity respectively. Groundwater storage, percolation and groundwater coefficients were assumed based on literature values (Ouédraogo *et al.*, 2018) as sub-daily discharge data of storm events was not available.

The Transform Method represents the conversion of the effective rainfall into a direct surface runoff after reducing all the losses such as infiltration, canopy storage, surface storage and evaporation. The Clark Unit hydrograph transform method represents two basic features of the rainfall-runoff process of the drainage basin. They are translation and attenuation which are represented by two parameters, time of concentration (T_c) and storage coefficient (R).

Infiltration and percolation volumes calculated using the soil moisture accounting method are considered as the inflow into the linear reservoir model to simulate the baseflow. All the parameters under the linear reservoir method were assumed based on literature values (Ouédraogo *et al.*, 2018) and they were later calibrated to achieve a satisfactory goodness of fit.

Calibration and Validation of the model

The model was calibrated for the period 1988-1993 by comparing the discharge simulation results with GloFAS discharges and with the calculated DAHITI and KMFRI discharges. The calibrated parameters were validated for the period 1994-2000 by comparing the simulation results against the corresponding GloFAS data and results were compared against DAHITI and KMFRI discharges.

Performance Indicators

The Omo basin is very large in extent and the parameters used in the hydrological model are averaged for the entire basin in the lumped model. Therefore, general performance indicators such as maximum, mean, standard deviation, 10th percentile, 50th percentile, 90th percentile and the coefficient of determination (R^2) were used to assess the goodness of fit of the simulated results during calibration and validation.

3.2.2. Semi-Lumped Model

Using the calibrated values from the lumped model as initial values, a semi-lumped hydrological model was developed by defining ten more sub-basins of the Omo basin. Sub-basins were defined particularly at the locations of Gibe I, II and III so that these reservoir performances can be simulated using the upgraded semi-lumped model. The reservoirs were defined as outlets for the sub-basins. HEC-HMS can represent reservoirs and their characteristics in terms of the inflow rates from the upstream and storage-outflow curves of the reservoirs. Hence, the model uses the input data and reservoir geometry characteristics to simulate the outflow. Figure 5 shows a schematic representation of the model setup in HEC-HMS where the 'junction tool' has been used to converge the flow from the sub-basins in the base model developed before considering the reservoirs.

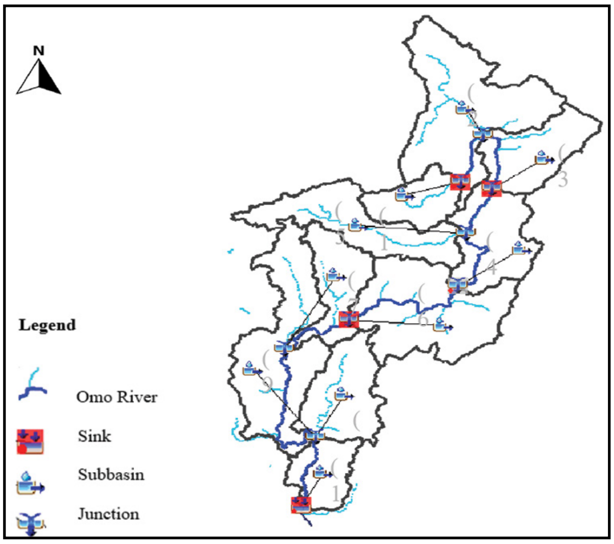

Fig. 5. Representation of the sub-basins of the Omo basin in HEC-HMS.

The semi-lumped model was set up using the same methods as in the lumped model to represent the hydrological processes (i.e. canopy, surface, loss, transform and linear reservoir routing).

The precipitation was input as a grid in the meteorological model in HEC-HMS to increase the accuracy of the hydrological model by considering the spatial variability of the precipitation data of the Omo Basin. CHIRPS data was used as MSWEP data format cannot be inserted in HEC-HMS as a precipitation grid.

Each sub-basin of the semi-distributed Omo basin was calibrated for the period 1988-1993 and validated for the period 1994-2000 using GloFAS discharge data.

Performance Indicators

As the spatial variation of the basin characteristics (such as *e.g.* canopy storage, impervious percentage, surface storage, and time of concentration) of the Omo basin were considered in the semi-lumped hydrological model, the results were relatively improved. Therefore, a more precise performance indicator, Nash Sutcliffe efficiency coefficient (*NSE*), was used to assess the goodness of fit of the model simulations during calibration and validation. The Nash Sutcliffe efficiency (*NSE*) equation is given by equation (2).

$$NSE = 1 - \frac{\sum_{t=1}^{T}(Q_0^t - Q_m^t)^2}{\sum_{t=1}^{T}(Q_0^t - \bar{Q}_0)^2} \qquad (2)$$

where $\bar{Q}_0$ is the mean of the observed discharges, $\bar{Q}_m$ is the modelled discharge and Q_0^t is the observed discharge at time *t*.

Assessing the impact of reservoirs

The semi-lumped model was further improved by incorporating the Gibe I, Gibe II, and Gibe III reservoirs. A continuous daily simulation was carried out for 2016-2019 to consider the impact of the reservoirs on the lake's shoreline and the water level. Gibe IV was not considered in the simulations due to the lack of data availability. The specific simulated releases in HEC-HMS were done as daily outflows from the reservoir, which were obtained under the assumption that these are equal to the sum of the environmental flow (17 m^3/s) and design outflow for the hydropower plant (101.5 m^3/s) (Theobald, 2016). The elevation-storage curve mentioned by Asefa (2011) and the elevation-outflow mentioned by Theobald (2016) discharge curves were used to derive the storage discharge curves for Gibe I and Gibe III (Fig. 6). For Gibe II monthly outflow discharge curves of Asefa (2011) were used.

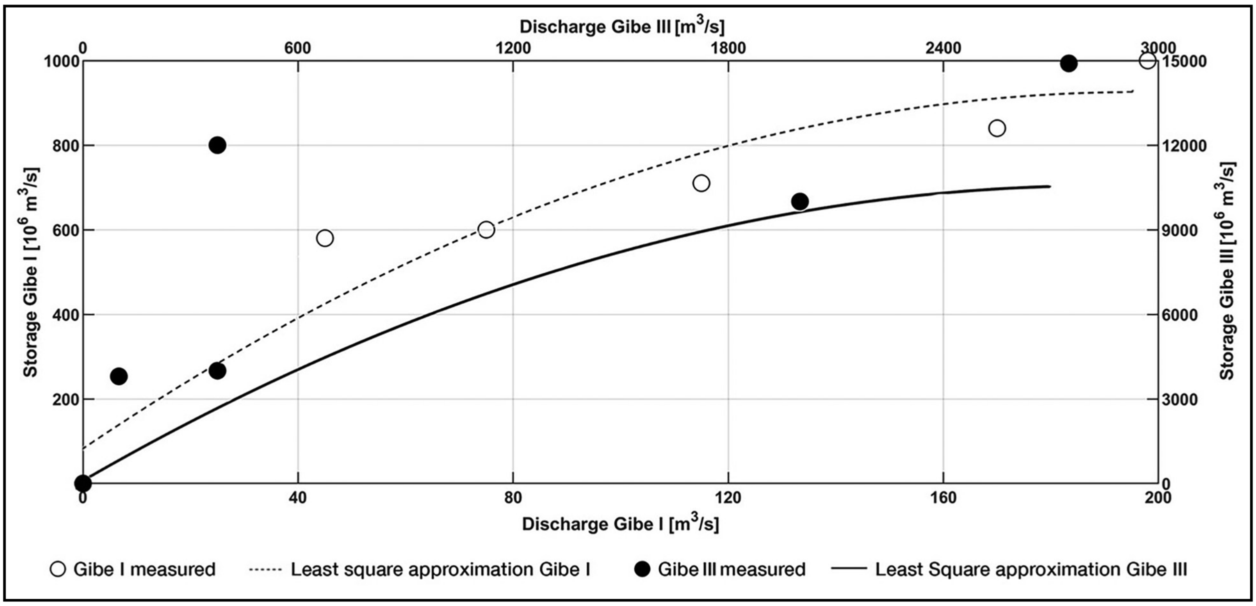

Fig. 6. Storage-Outflow relationship estimations for GibeI and Gibe III (measured points from Theobald, 2016).

3.3. Lake water level variation modelling

A lake water level variation model was built to assess the impact of upstream conditions on the variation of the shoreline and the water level of the lake. The bathymetry of the lake was developed based on the contour map obtained from Avery and Tebbs (2018). This bathymetry was overlaid on the digital elevation model to represent the elevation variation of the study area. The lake water level variation model was developed using the model builder tool in ArcGIS which considers the initial water level, cumulative inflow volumes for intervals of ten days and rainfall on the lake surface as input to the model. The only outflow from the lake, evaporation, was deducted as a volume by multiplying the constant evaporation (7.2 mm/day) by the surface area of each time step using the area-elevation curve.

The obtained volumes are converted to altimetry heights using the elevation-volume relationship derived from the bathymetry, represented in Figure 7. The shoreline maps were obtained using the derived altimetry heights for each increment of ten days.

The obtained shoreline variation maps were compared against satellite imagery of the lake for the corresponding date to validate the water level variation model by visually inspecting the results. Satellite imagery of the lake was obtained by deriving the Normalized Difference Water Index (NDWI) using green and Near Infrared (NIR) bands of Landsat 5 and Landsat 7 of the NASA/USGS program. This analysis was carried out for the year 2000. The equations used for the calculation of the *NDWI* are illustrated in equation 3 and 4:

$$NDWI = \frac{(Green\ band - Near\ Infrared\ Band)}{(Green\ band + Near\ Infrared\ Band)} \quad (3)$$

$$NDWI = \frac{(Band\ 2 - Band\ 4)}{(Band\ 2 + Band\ 4)} \quad (4)$$

The validated semi-lumped hydrological model and the water level variation model were used to assess the impact on the lake water level due to two scenarios. The two scenarios modelled the lake water level variation due to rainfall from three consecutive wettest years and driest years when the lake water level is initially at the recorded lowest level (354.91 m.a.s.l on 7/15/1988) (Scenario A) and the highest water levels (365.57 m.a.s.l on 12/15/1998) (Scenario B).

4. RESULTS AND DISCUSSIONS

4.1. Hydrological Model Simulations

4.1.1. Lumped Model

Calibration of the Model

The simulation results and the parameters obtained for the Omo basin during calibration are illustrated in the Figure 8 and Table 2 respectively. The continuous simulation was carried out at daily time intervals. The simulated results and the KMFRI back-calculated discharges were converted to monthly average discharges to compare with monthly discharges obtained from Avery (2010). The general pattern of the discharge shows peak discharges during August- September, corresponding to the wet season. The obtained discharges tend to maintain the pattern although KMFRI discharges show an abnormality in the peaks in the year 1990. On the contrary, obtained data show a drastic increment during the year 1992 while the KMFRI discharges and simulated discharges follow a similar pattern. The Arid Lands Resource Management Project has declared the year 1992 as one of the "Nine droughts recorded in Kenya in the last 40 years" and such high discharge peaks have not been recorded in lakes such as Lake Tana which is located in the vicinity of Lake Turkana. In conclusion the model has been able to successfully simulate low flows and a few peaks that have occurred during the wet season in July-August.

Validation of the model

The model was run from 1994 to 2000 using the calibrated parameters and the results obtained were compared against DAHITI and KMFRI calculated discharges.

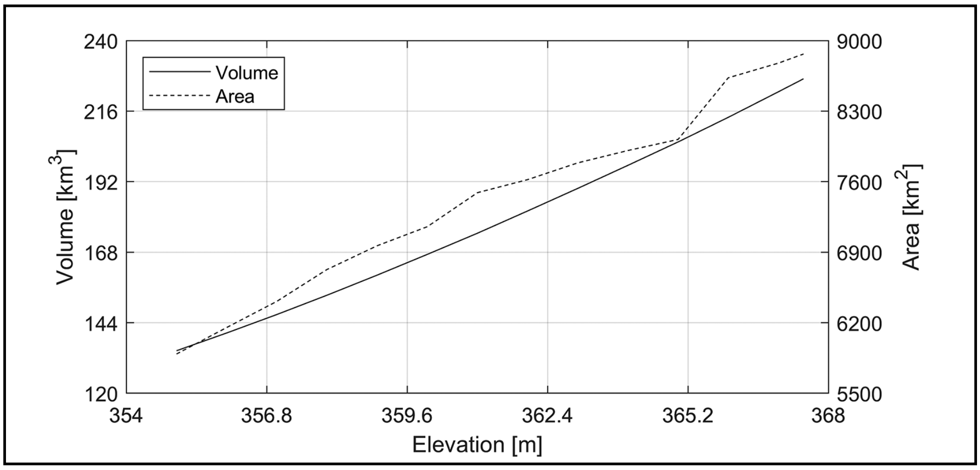

Fig. 7. Volume-Area-Elevation curves for lake Turkana.

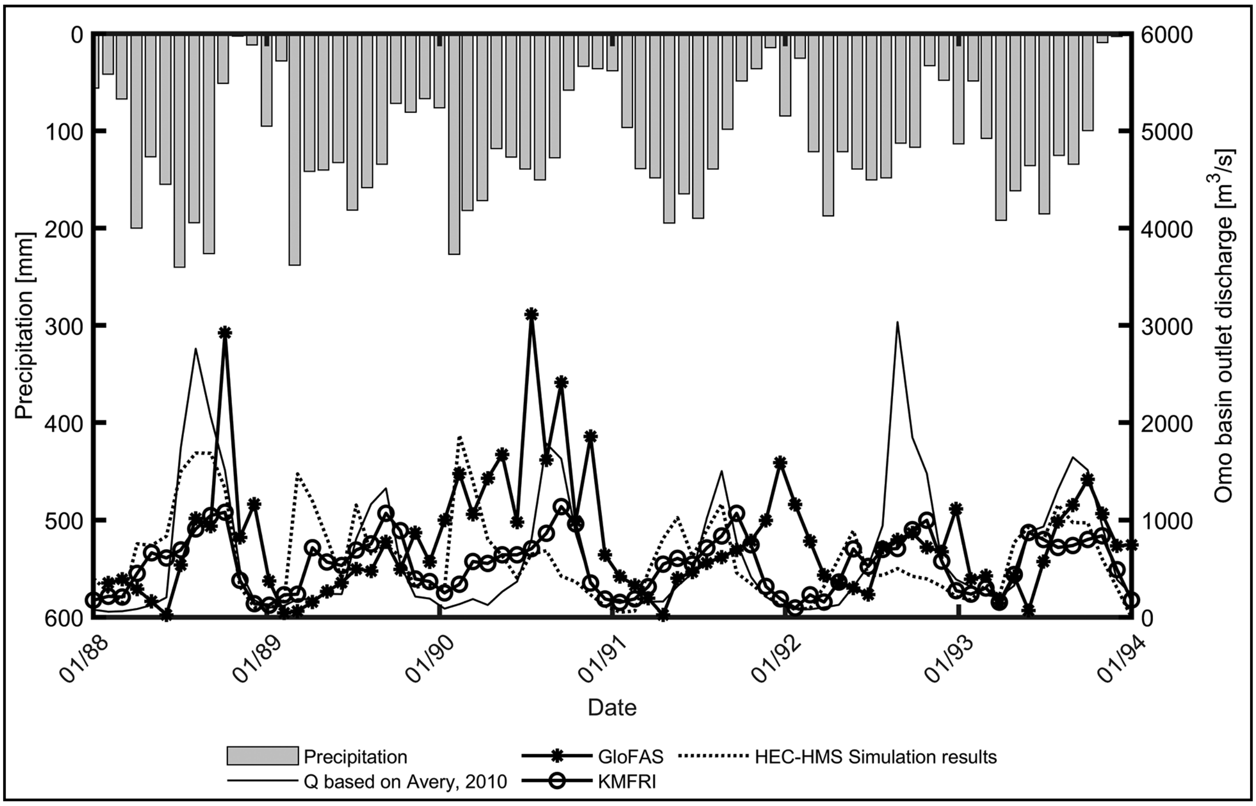

Fig. 8. Calibration results of the lumped model at monthly scale.

Table 2. Performance indicators for the calibration and validation of the lumped model

	HEC-HMS Simulation	KMFRI Data	Literature Data	GloFAS Data
Performance indicators for calibration (1988-1993)				
Min Q (m^3/s)	58.6	4.7	57.0	95.8
Max Q (m^3/s)	1873.7	3071.7	3035.0	1137.3
Mean Q (m^3/s)	626.4	792.2	637.5	546.6
Std. Deviation (m^3/s)	445.9	635.5	671.9	288.1
10^{th} Percentile (m^3/s)	126.4	231.0	101.0	175.8
50^{th} Percentile (m^3/s)	482.1	714.6	320.0	560.6
90^{th} Percentile (m^3/s)	1204.3	1589.4	1629.0	944.4
R^2		0.2	0.4	0.5
Performance indicators for Validation (1994-2000)				
Min Q (m^3/s)	9.5	22.9	68.7	56.9
Max Q (m^3/s)	3664.4	3168.3	2313.0	1352.9
Mean Q (m^3/s)	674.4	701.1	989.2	565.4
Std Deviation (m^3/s)	720.7	532.4	518.7	344.2
10^{th} Percentile (m^3/s)	77.7	235.8	336.1	103.9
50^{th} Percentile (m^3/s)	447.7	595.3	988.6	566.0
90^{th} Percentile (m^3/s)	1414.9	1278.8	1713	1045.0
R^2		0.3	0.3	0.4

The simulation carried out to validate the model shows similar characteristics where the low flows are simulated considerably well compared to the high flows. The model simulates the seasonal variation with a uni-modal pattern. However, the simulated results show two peaks for the year 1997 due to extreme rainfall events (in May and November) and 1997 is not reflected in the back-calculated discharges. Due to the high uncertainty in simulated results and the back-calculated results, a semi-distributed model was developed using gridded precipitation data. Results shows correlation with GloFAS data.

4.1.2. Semi-Lumped Model

Calibration of the model

The calibrated semi-lumped model has improved significantly compared to the lumped model and has been able to simulate the flow satisfactorily except for the peak discharge during the wet season (Fig. 9a). Therefore, the simulated discharges are underestimated. However, the seasonal variation of the discharge is well simulated, and the discharge pattern is maintained.

Validation of the model

The calibrated parameters were used to validate the semi-lumped model by simulating the flow for the years 1994-2000. Similar to the calibration period, the low flows were well simulated while the peak discharges were underestimated Figure 9b. The Nash-Sutcliffe coefficient was used to assess the goodness-of-fit of the simulated and the observed discharges. The main reason behind selecting this performance indicator is because the results have improved in the semi-lumped model compared to the lumped model and the simulations are carried out on a daily scale. Table 3 illustrates the coefficients obtained for each sub-basin for calibration and validation.

Assessing the impact of reservoirs

Figure 10 presents the results obtained between 2016 and 2019 in terms of the Omo basin inflow into the lake, as well as the corresponding lake water level variation.

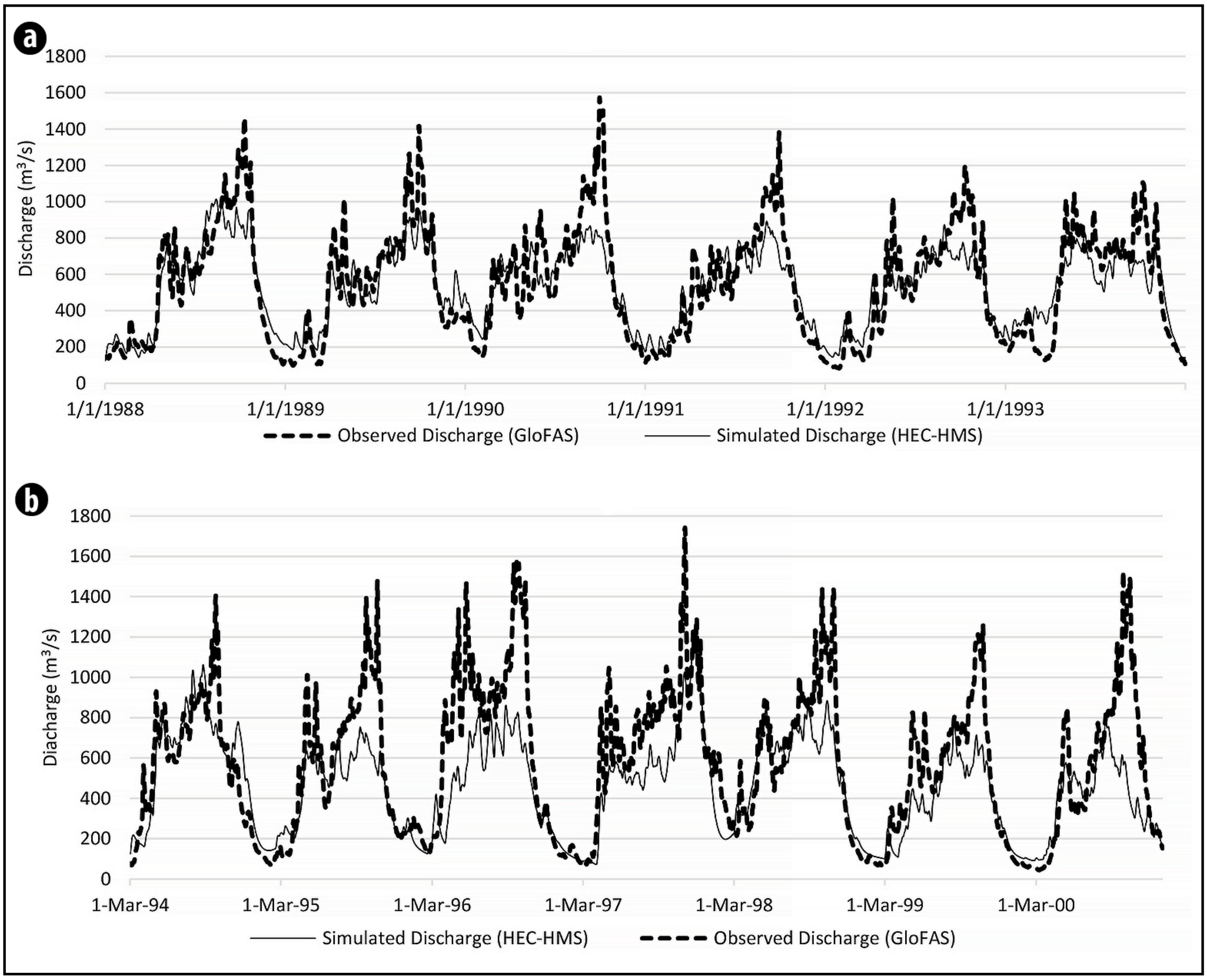

Fig. 9. (**a**) Calibration results of the semi-lumped model at the outlet (lake) on a daily scale, (**b**) Validation results of the semi-lumped model at the outlet (lake) on a daily scale.

Table 3. Goodness of fit (NSE) during calibration and validation

Sub-basins of the Omo basin	Calibration	Validation
1	0.88	0.71
2	0.89	0.77
3	0.77	0.69
4	0.79	0.67
5	0.56	0.56
6	0.70	0.69
7	0.46	0.56
8	0.41	0.23
9	0.73	0.64
10	0.76	0.53

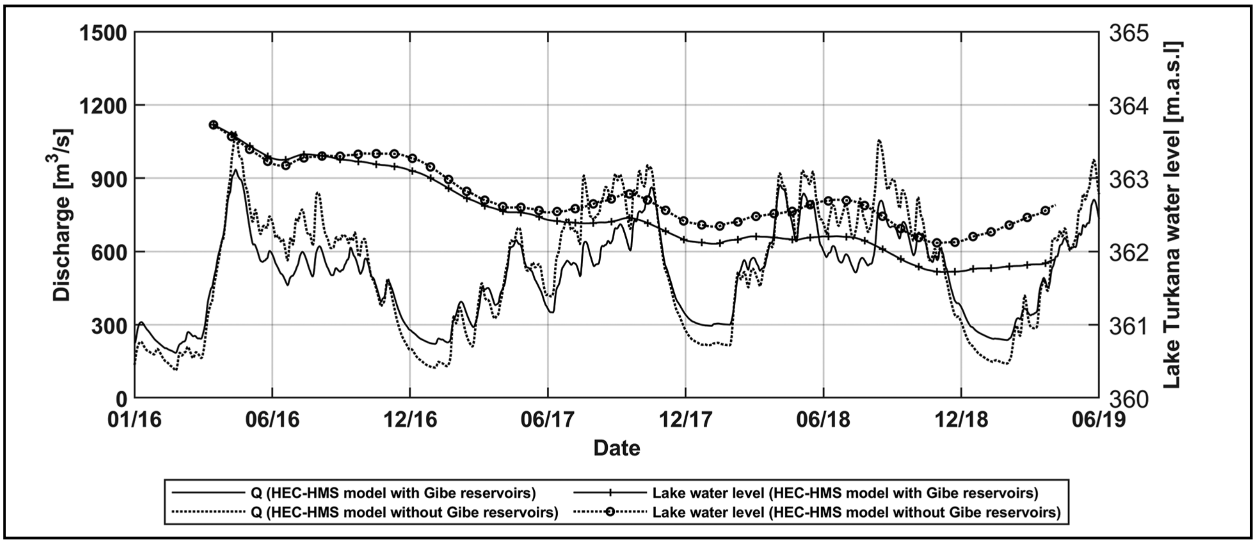

Fig. 10. Simulated Omo basins daily discharge and the corresponding lake water level variations, with and without the impact of reservoirs.

The results show a slight increase in the low flows and a decrease in high flows because of the functioning of the reservoirs. According to the water level variation model simulation, the overall impact on the lake level is that it is expected to decline due to the influence of the reservoirs on the Omo River discharge.

4.2. Lake water level variation modelling

The developed water level variation model results were compared with water extent area obtained from Landsat 5 and Landsat 7 images for the year 2000 (Fig. 11). By visually analyzing the results, it can be seen that there is an overestimation of the shoreline area at the South end of the lake and an underestimation of the extent at the North end of the lake. Furthermore, the three islands of the lake are not simulated as significantly as in the water area obtained from the satellite image. However, the model has succeeded to simulate the general shape and extent of the lake's shoreline. A reason for the shift in the results could be because the satellite imagery does not correspond to the exact date of the simulation results as the satellite imagery did not produce images of the lake at a constant frequency. Table 4 shows the dates corresponding to the satellite imagery and each simulation result. Therefore, a significant change in the shoreline area was not observed every ten days. This did not allow for assessing the model performance, therefore, a scenario was simulated that checks the water level variation at an inundation levels of 368.8 m.a.s.l. and 364 m.a.s.l. The water levels generated by the water level variation model were compared with DAHITI and KMFRI altimetry heights as shown in Figure 12. It can be observed that the simulated water levels maintain the decrease in the water level until mid-2000 but it does not show the increase in the water level during the later years of the simulation as significantly as DAHITI data but it maintains the pattern of KMFRI altimetry heights during the later years.

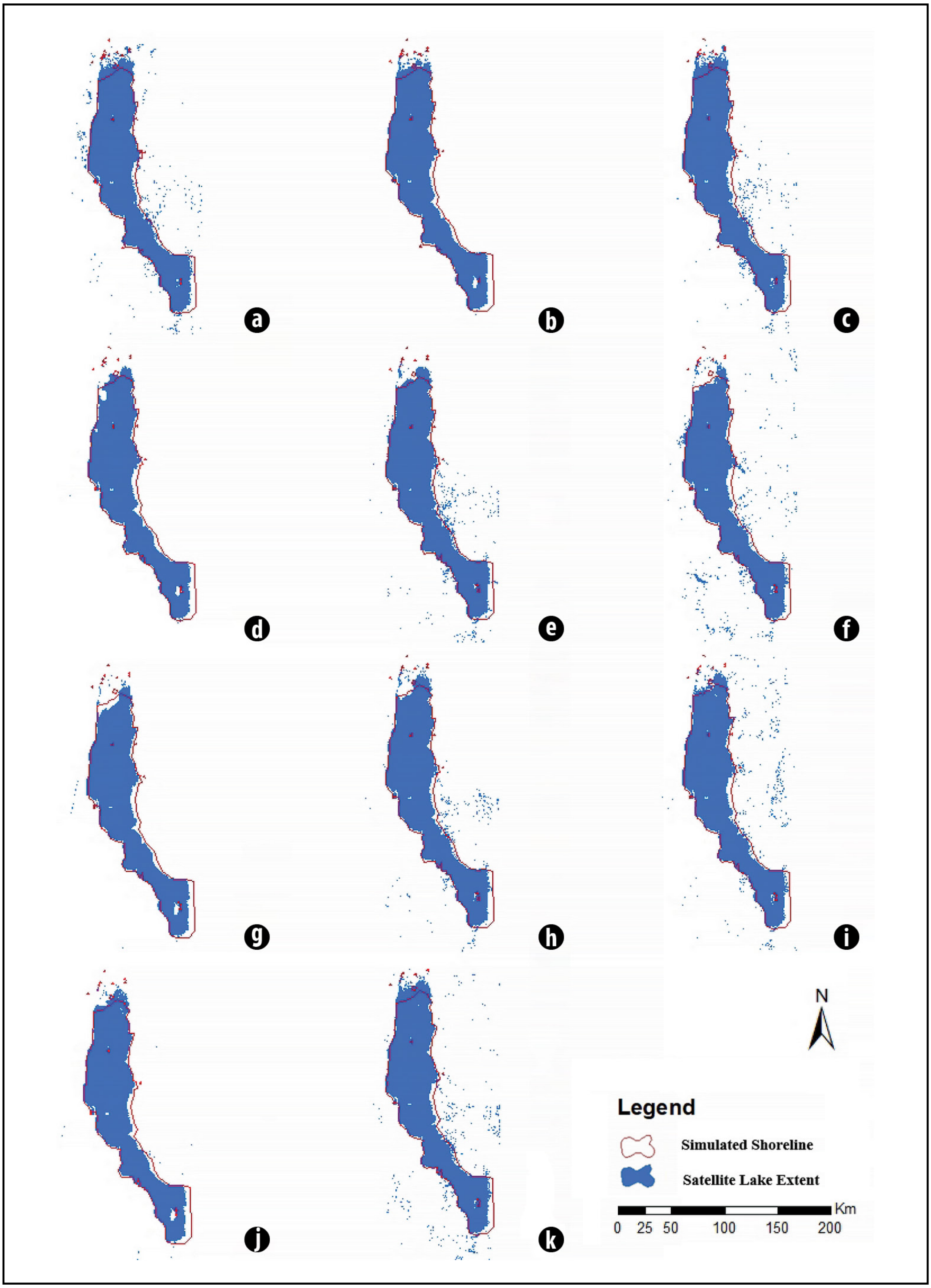

Fig. 11. Comparison of the results obtained from the lake water level model with satellite data.

Table 4. Dates corresponding to simulation results and satellite imagery (related to Figure 11)

Simulation	Date of the satellite Imagery	Date of simulation results
(a)	30/01/2000	04/02/2000
(b)	12/02/2000	09/02/2000
(c)	20/02/2000	19/02/2000
(d)	18/05/2000	19/05/2000
(e)	13/07/2000	08/07/2000
(f)	29/07/2000	28/07/2000
(g)	06/08/2000	07/08/2000
(h)	30/08/2000	27/08/2000
(i)	01/10/2000	06/10/2000
(j)	25/10/2000	26/10/2000
(k)	20/12/2000	25/12/2000

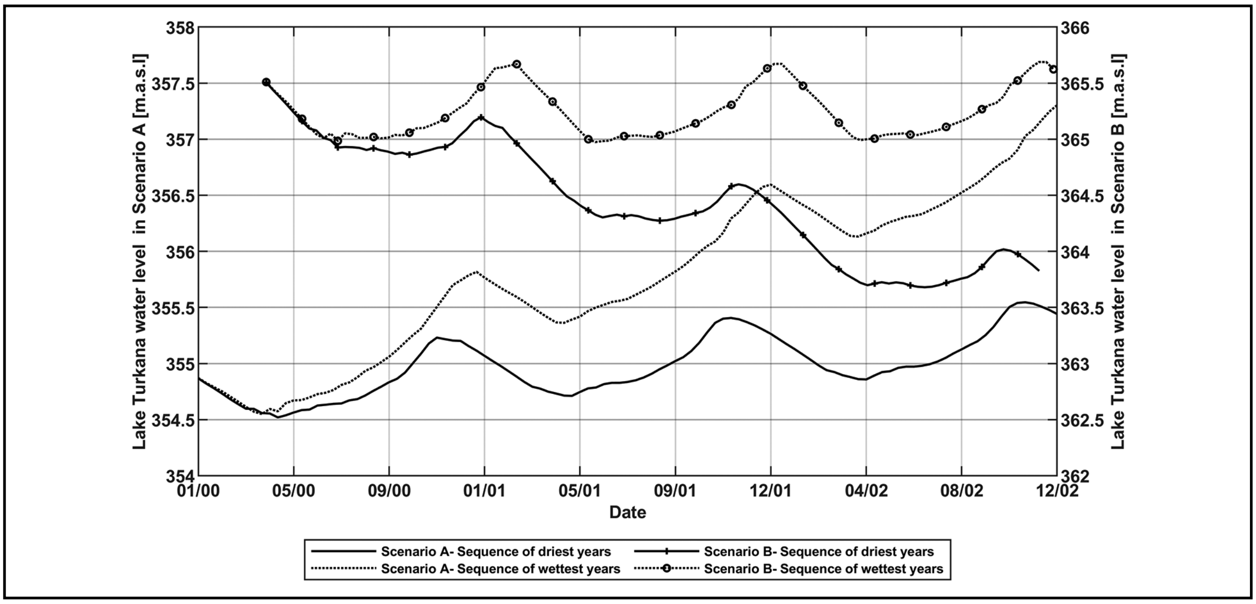

Fig. 12. Results of the scenario modelling: Scenario A and Scenario B with the wettest hydrological year and the driest hydrological year.

4.3. Hydrological conditions scenario modelling

Two hydrological conditions scenarios, wet and dry, were modelled using the semi-lumped model without considering the reservoirs. Two initial levels in the lake were considered: the lowest recorded level (Scenario A) and the highest recorded level (Scenario B). Figure 12 illustrates results obtained when the model was run with the lake water level at its lowest recorded elevation (354.9 m.a.s.l.) and it can be seen that the trend in the water level variation is an increasing one for both the wettest and driest period (of three years) inflows. Due to the wettest annual rainfall, the overall increment of the lake level by the end of the three years wet period is over 3 meters. However, the increment of the lake level by the end of the three driest years, in scenario A, is only less than 1 meter. This is because the volume of water during the three consecutive wettest years is very much higher than that of the three consecutive driest years.

Similar to Scenario A, Scenario B shows an overall decrease of over 1 meter in the water level during the driest years since the evaporation is very high when the lake's water level is high due to the increased lake surface. This theory can be further validated by analyzing Scenario B where the increase of the lake water level is only 0.2 m during the wettest years when the lake's initial water level is very high as previously the increase was over 3 m for the wettest years when the lake's initial water level was the lowest.

The reason for the overall increment of the water level of scenario A is that when the lake water level is low, the surface area is low. Since the surface area is low, the area from which the evaporation takes place is low. This will lead to a lesser loss due to evaporation compared to lake inflows. This will result in an overall increase in the lake water level for Scenario A. Wise versa for Scenario B when the initial level of the lake is high, the surface area is large. Therefore, the loss due to evaporation is higher than the lake inflows. As a result, the lake water level will decline (during the driest years) or slightly increase (during the wettest years).

5. CONCLUSIONS

This research study was carried out to identify the relevant globally available data, which combined with limited available in-situ data can be used for developing a rainfall-runoff model of the Lake Turkana Basin and a follow-up Lake Turkana model. These models should serve as tools for simulating and analyzing different impact scenarios. To address the research questions, this study developed three main models: two hydrological models based on HEC-HMS and a water level variation based on ArcGIS. The two hydrological models were a lumped one, developed to get an understanding of the catchment characteristics; and a semi-lumped one. The semi-lumped hydrological model was based on the lumped model, modified to incorporate the three reservoirs Gibe I, Gibe II and Gibe III. Therefore, this hydrological model can be used to simulate different scenarios by altering external factors of the Omo basin to assess the impact on the Turkana lake water level.

In the analysis of the results, it was observed that the results from the semi-lumped model showed a higher goodness of fit compared to the lumped model. This was because the spatial variation of the input parameters (including the precipitation as a grid) was considered in the semi-lumped model. Also, when the results of the calibrated semi-lumped model with reservoirs were studied, it was observed that the water level of the lake has declined approximately by 0.7 m due to the impact of the three reservoirs for the years 2015-2019. The lake variation model was overestimating the shoreline area of the lake at the northern end and underestimated the shoreline area of the lake at the southern end. This could be due to the lag in the dates of comparison and uncertainties in data (satellite image classification and simulated inflow data). According to the comparison between simulated and literature data, it is confirmed that the water level variation managed to simulate the inundation of the settlements similar to the literature.

As Lake Turkana is an ungagged lake that does not have measured data freely accessible to the public, this study investigated available remotely sensed and freely available data to develop the hydrological model and the water level variation. For the hydrological model, globally available data such as SSURGO was used for soil maps and Global Land Cover Characterization (GLCC) for Land Cover Classification. Initially, MSWEP rainfall data was used in the development of the lumped model. However, CHIRPS data was used in the semi-lumped model as the MSWEP data format cannot be used in the HEC-HMS when considering precipitation as a gridded input. The analysis carried out to compare MSWEP and CHIRPS data showed similar patterns in the two data sets which allowed using the two datasets interchangeably. During the calibration and the validation of the lumped hydrological model, DAHITI remote sensed altimetry heights were used to compare validated results. However, the back-calculated discharges from DAHITI did not deliver satisfactory results. In addition, DAHITI altimetry heights showed differences in its data when compared with KMFRI measured altimetry heights. Moreover, as discussed under Section '3.1', there is enough evidence that KMFRI measures altimetry heights have recorded errors as well. As a result, DAHITI and KMFRI data were not very useful during the development of the two hydrological models. However, satisfactory results were obtained using the semi-lumped model as it was calibrated and validated using GloFAS discharge data. It can be concluded that the aforementioned globally available data can be used to carry out a study for Lake Turkana. It could also be concluded that the main limitation of remotely sensed data is the significant uncertainty associated with the data and the unavailability of such data in the required format or frequency.

Two scenarios (Scenario A and Scenario B) based on initial conditions of the lowest (354.91 m.a.s.l.) and highest (365.57 m.a.s.l.) recorded water levels were modelled using the developed semi-lumped hydrological model and the water level variation model. It was observed that the water level tends to decrease or increase slightly due to lake inflows when the initial condition of the lake is at the highest recorded water level since the evaporation is high at high water levels. Similarly, it was observed that when the lake's initial water level is low, the lake's level increased drastically for the wettest years and increased slightly for the driest years as the evaporation is much lower when the initial condition of the lake is at the lowest recorded level. Thus, the equilibrium of the lake's water level will be maintained. Finally, it can be concluded that the semi-lumped hydrological model and the Lake Turkana model can be used to model various scenarios and assess their impacts on the lake's water level.

ACKNOWLEDGEMENTS

We would like to thank to the Dutch Ministry for Foreign Affairs' Water, Peace and Security (WPS) partnership for providing the necessary literature to get a proper understanding of the case study. This research did not receive any specific grant from funding agencies in the public, commercial, or not-for-profit sectors.

REFERENCES

Ali, M.H., Popescu, I., Jonoski, A., Solomatine, D.P. (2023). Remote Sensed and/or Global Datasets for Distributed Hydrological Modelling: A Review. *Remote Sens*., **15**: 1642. https://doi.org/10.3390/rs15061642

Asefa, D. (2011). Water Use and Operation Analysis of Water Resource Systems in Omo Gibe River Basin. Addis Ababa University.

Avery, S.T. (2010). Hydrological Impacts of Ethiopia's Omo Basin on Kenya's Lake Turkana Water Levels & Fisheries. Tunis.

Avery, S.T., Tebbs, E.J. (2018). Lake Turkana, major Omo River developments, associated hydrological cycle change and consequent lake physical and ecological change. *Journal of Great Lakes Research*, **44**(*6*): 1164-1182. Doi: 10.1016/j.jglr.2018.08.014

Boës, X., Prat, S., Arrighi, V., Feibel, C., Haileab, B., Lewis, J., Harmand, S. (2019). Lake-level changes and hominin occupations in the arid Turkana basin during volcanic closure of the Omo River outflows to the Indian Ocean. *Quaternary Research* (United States), **91**(*2*): 691-704. Doi: 10.1017/qua.2018.118

Carr, C.J. (2017). River Basin Development and Human Rights in Eastern Africa - A Policy Crossroads. River Basin Development and Human Rights in Eastern Africa - A Policy Crossroads. Doi: 10.1007/978-3-319-50469-8

Cerling, T.E., Yuretich, R.F. (1983). Hydrogeochemistry of Lake Turkana, Kenya: Mass balance and mineral reactions in an alkaline lake. *Geochimica et Cosmochimica Acta*, **47**(*6*): 1099-1109.

Chen, J., Li, Z., Li, L., Wang, J., Qi, W., Xu, C.Y., Kim, J.S. (2020). Evaluation of multi-satellite precipitation datasets and their error propagation in hydrological modeling in a monsoon-prone region. *Remote Sensing*, **12**(*21*): 1-33. Doi: 10.3390/rs12213550

Christopher, A. (2014). Paleohydrology of Lake Turkana and its influence on the Nile River system. Palaeogeography, palaeoclimatology, palaeoecology.

Climate Hazards Center (2022). CHIRPS: Rainfall Estimates from Rain Gauge and Satellite Observations. Retrieved June 28, 2022, from https://www.chc.ucsb.edu/data/chirps

Earth Resources Observation and Science (EROS) Center. (2018). SGS EROS Archive - Land Cover Products - Global Land Cover Characterization (GLCC). https://www.usgs.gov/centers/eros/science/usgs-eros-archive-land-cover-products-global-land-cover-characterization-glcc#:~:text=Global Land Cover Characterization (GLCC) is a series of global (Normalized Difference Vegetation Index) composites.

ECMWF (2020). OpenIFS: Surface Model HTESSEL. Retrieved from https://confluence.ecmwf.int/display/OIFS/3.3+OpenIFS%3A+Surface+Model+HTESSEL (last accessed on October 20, 2023).

Flemming, M. (2002). Continuous Hydrologic Modelling with HMS: Parameter Estimation and Model Calibration and Validation.

GloH20 (2022). GloH20. Retrieved June 29, 2022, from http://www.gloh2o.org/mswep/

Gownaris, N.J., Pikitch, E.K., Aller, J.Y., Kaufman, L.S., Kolding, J., Lwiza, K.M.M. (2017). Fisheries and water level fluctuations in the world's largest desert lake. *Ecohydrology*, **10**(*1*). Doi:10.1002/eco.1769

Grekousis, G., Mountrakis, G., Kavouras, M. (2015). An overview of 21 global and 43 regional land-cover mapping products. *International Journal of Remote Sensing*, **36**(*21*): 5309-5335. Doi: 10.1080/01431161.2015.1093195

Haack, B. (1996). Monitoring wetland changes with remote sensing: An east African example. *Environmental Management*, **20**(*3*): 411-419. Doi: 10.1007/BF01203848

HEC-HMS User's Manual (2022). HEC-HMS User's Manual. US Army Corps of Engineers Hydrologic Engineering Center.

Johnson, T.C., Malala, J.O. (2009). Lake Turkana and Its Link to the Nile. *Monographiae Biologicae*, **89**: 287-304. DOI: 10.1007/978-1-4020-9726-3_15

Kolding, J. (1992). A summary of Lake Turkana: An ever-changing mixed environment. *SIL Communications, 1953-1996*, **23**(*1*): 25-35. Doi: 10.1080/05384680.1992.11904005

Loveland, T.R., Reed, B.C., Brown, J.F., Ohlen, D.O., Zhu, J., Yang, L., Merchant, J. (2000). Global Land Cover Characteristics Data Base Version 2.0. *International Journal of Remote Sensing*, **21**(*6/7*): 1303-1330.

Miriti, E.A.K. (2017). African Great Lakes. Retrieved June 30, 2022, from https://www.africangreatlakesinform.org/article/lake-turkana#:~:text=The Lake Turkana fishery is, the population around the lake.

Muška, M., Vašek, M., Modrý, D., Jirků, M., Ojwang, W.O., Malala, J.O., Kubečka, J. (2012). The last snapshot of natural pelagic fish assemblage in Lake Turkana, Kenya: A hydroacoustic study. *Journal of Great Lakes Research*, **38**(*1*): 98-106.

Musa, Z.N., Popescu, I., Mynett, A. (2015). A review of applications of satellite SAR, optical, altimetry and DEM data for surface water modelling, mapping and parameter estimation, *Hydrol. Earth Syst. Sci.*, **19** (*9*): 3755-3769, DOI: 10.5194/hessd-12-4857-2015

NASA (2022). U.S. Releases Enhanced Shuttle Land Elevation Data.

Obiero, K., Donde, O., Gownaris, N., Pikitch, E.K. (2016). The Wetland Book. The Wetland Book, (July 2018). Doi: 10.1007/978-94-007-6173-5

Ouédraogo, W.A.A., Raude, J.M., Gathenya, J.M. (2018). Continuous modeling of the Mkurumudzi River catchment in Kenya using the HEC-HMS conceptual model: Calibration, validation, model performance evaluation and sensitivity analysis. *Hydrology*, **5**(*3*). Doi: 10.3390/hydrology5030044

Schwatke, C., Dettmering, D., Bosch, W., Seitz, F. (2015). DAHITI - An innovative approach for estimating water level time series over inland waters using multi-mission satellite altimetry. *Hydrology and Earth System Sciences*, **19**(*10*): 4345-4364 Doi: 10.5194/hess-19-4345-2015

Sedano, F., Gong, P., Ferrão, M. (2005). Land cover assessment with MODIS imagery in southern African Miombo ecosystems. *Remote Sensing of Environment*, **98**(*4*): 429-441. Doi: 10.1016/j.rse.2005.08.009

Theobald, S. (2016). Modelling of Cascade Dams and Reservoir Operation for Optimal Water Use: Application to Omo Gibe River Basin, Ethiopia. Kassel University.

United Nations Environment Programme (2020). Lake Turkana and its River Basins. Retrieved July 6, 2023, from https://watertools-portal.azurewebsites.net/ portal/workspaces/lake+turkana+and+its+river+basins

United Nations Environment Programme (2012). Ethiopia's GibE iii Dam its potEntial impact on Lake Turkana Water Level.

USDA (2022). Natural Resources Conservation Service Soils. Retrieved from https://www.nrcs.usda.gov/wps/portal/nrcs/detail/soils/survey/?cid=nrcs142p2_053627 (last accessed on October 6, 2023).

USGS (2022). Gibe III Dam. Retrieved August 1, 2022, from https://eros.usgs.gov/media-gallery/earthshot/gibe-iii-dam#:~:text=At nearly 244 meters tall,is 6%2C500 GWh a year

Velpuri, N.M., Senay, G.B., Asante, K.O. (2012). A multi-source satellite data approach for modelling Lake Turkana water level: Calibration and validation using satellite altimetry data. *Hydrology and Earth System Sciences*, **16**(*1*): 1-18. Doi: 10.5194/hess-16-1-2012

van der Knijff, J.M., Younis, J., de Roo, A.P.J. (2010). LISFLOOD: A GIS-based distributed model for river basin scale water balance and flood simulation. *International Journal of Geographical Information Science*, **24**(*2*): 189-212. Doi: 10.1080/13658810802549154

van der Lubbe, H.J.L., Krause-Nehring, J., Junginger, A., Garcin, Y., Joordens, J.C.A., Davies, G.R. (2017). Gradual or abrupt? Changes in water source of Lake Turkana (Kenya) during the African Humid Period inferred from Sr isotope ratios. *Quaternary Science Reviews*, **174**: 1-12 Doi: 10.1016/j.quascirev.2017.08.010